IOPscience iopscience.iop.org

Home Search Collections Journals About Contact us My IOPscience

Growth of nanostructures on composition-modulated InAlAs surfaces

This article has been downloaded from IOPscience. Please scroll down to see the full text article.

2004 J. Phys.: Condens. Matter 16 7603

(http://iopscience.iop.org/0953-8984/16/43/004)

View the table of contents for this issue, or go to the journal homepage for more

Download details:
IP Address: 129.252.86.83
The article was downloaded on 27/05/2010 at 18:22

Please note that terms and conditions apply.

INSTITUTE OF PHYSICS PUBLISHING JOURNAL OF PHYSICS: CONDENSED MATTER

J. Phys.: Condens. Matter **16** (2004) 7603–7610 PII: S0953-8984(04)76016-6

Growth of nanostructures on composition-modulated InAlAs surfaces

F A Zhao, Y H Chen, X L Ye, P Jin, B Xu, Z G Wang and C L Zhang

Key Laboratory of Semiconductor Materials Science, Institute of Semiconductors, Chinese Academy of Sciences, PO Box 912, Beijing, People's Republic of China

E-mail: zhaofa@red.semi.ac.cn

Received 11 February 2004, in final form 9 September 2004
Published 15 October 2004
Online at stacks.iop.org/JPhysCM/16/7603
doi:10.1088/0953-8984/16/43/004

Abstract
InAs self-organized nanostructures were grown with variant deposition thickness and growth rate on closely matched InAlAs/InP by molecular-beam epitaxy. The structural properties of InAs and InAlAs layer were studied. It is found that the InAs morphology is insensitive to the growth conditions. Transmission electron microscopy and reflectance difference spectroscopy measurements show that the InAlAs matrix presents lateral composition modulation which gives birth to surface anisotropy. Based on the dependence of the InAs morphology on the anisotropy of the InAlAs layer, a modified Stranski–Krastanow growth mode is presented to describe the growth of the nanostructure on a composition-modulated surface.

1. Introduction

InAs quantum dots (QDs) based on an InP substrate are a topic of great interest because their luminescence is in the technologically important wavelength region of 1.55 μm. In contrast to the InAs/GaAs system, the self-assembled InAs QDs formation process on an InP substrate is very complicated due to the weaker driven force from the lower misfit strain (3.2%), which means that the other factors, such as chemical alloying with the substrate, morphology and chemical instabilities of the alloy buffer layer, anisotropic surface diffusion, etc, may compete with the misfit strain and greatly affect the self-assembled process [1–4]. It has been shown that the morphology of the InAs nanostructures depends critically on the nature of the buffer layers [4]. InAs quantum wires (QWRs) are formed on the InAlAs buffer and QDs are formed on the InGaAs buffer. In some cases, a mixture of InAs QDs and QWRs can be formed on the InAlAs buffer layer [5, 6]. However, the influence of the alloy buffers on the morphology of the self-assembled nanostructures remain unclear. Previous studies indicate that InAlAs is an immiscible alloy; it usually produces lateral composition modulation (LCM) to reduce

© 2004 IOP Publishing Ltd Printed in the UK

the total free energy [7]. LCM in InAlAs film is demonstrated to be a misfit-driven kinetic process, initiated by random compositional fluctuations and amplified gradually with film deposition [7–9]. LCM is frequently observed in InAlAs epilayers grown on InP by the metal-organic chemical vapour deposition (MOCVD) technique [9, 10]. It has been reported that depositing InAs on such an InAlAs surface will make InAs grow under inhomogeneous strain distribution [11], which is beyond the original theory of the standard Stranski–Krastanow (SK) growth mode that occurs on a homogeneous surface. Although no LCM was reported for closely matched InAlAs/InP grown by the molecular beam epitaxy (MBE) technique, there is probably weak LCM in InAlAs epilayers grown under appropriate conditions, which plays an important role in the formation of nanostructures. In this work, we find that the morphology of self-assembled InAs nanostructures grown on closely matched InAlAs/InP(001) is insensitive to the InAs deposition thickness and growth rate. The insensitivity is attributed to the effect of the weak LCM in InAlAs epilayers, which is observed by transmission electron microscopy (TEM) measurements. In-plane optical anisotropy around the InAlAs band edge arising from the weak LCM is clearly observed by reflectance difference spectroscopy (RDS) measurements. It is found that high RD intensity corresponds to longer wires, which indicates a strong influence of the LCM on the InAs morphology. Based on the experimental results, a modified SK film growth mechanism is pictured for the growth of the nanostructures on a composition-modulated surface.

2. Experimental details

Our samples were grown on semi-insulating InP(001) substrates by a Riber32 MBE system. After oxide desorption, a 200 nm-thick $In_{0.52}Al_{0.48}As$ matrix layer was first grown at 510 °C with a growth rate of 0.7 μm h^{-1}. Then the substrate temperature was lowered to 500 °C, and the InAs was deposited. During growth, the As_4 partial pressure was kept at 1×10^{-7} Torr, and the V/III flux ratio was 15. Before and after the deposition of InAs, a 2 min annealing step at growth temperature was carried out, and the As flux was always opened until the temperature had fallen below 300 °C to ensure that no As was lost from the surface. For the samples designed for the PL measurements, an additional 50 nm InAlAs cap layer was grown. In order to prevent the In desorption, a 5 nm InAlAs layer was first grown at the same temperature as the InAs layer, and then the temperature was raised to 510 °C to grow the rest of the InAlAs. In each growth run, one of the InAs growth conditions was varied, while the rest were kept identical. The growth conditions varied were layer thickness and the growth rate. Besides the InAs coverage samples, a sample having only a 500 nm-thick InAlAs layer without InAs coverage was also grown for structure measurements.

3. Results and discussion

3.1. Structural properties

3.1.1. Structural properties of InAs nanostructures. The effect of the InAs layer thickness and the growth rate was studied by atomic force microscopy (Nanoscope 3 AFM, Digital Instruments) in-air in the contact mode. Figures 1(a)–(c) illustrate the variation of the surface morphology as a function of InAs layer thickness. The growth rate of InAs is 0.2 ML s^{-1}. In figure 1(a), the 3 ML-thick InAs layer forms a QWR aligned along the $[1\bar{1}0]$ direction, a spot of elongated bright QDs (the bright flecks) can be found on the wires. With the increase of the InAs thickness to 4 MLs, the QWR is still discernible in the background, while the number of the bright QDs formed on the wires increases as shown in figure 1(b). As for the 6 ML-thick InAs sample shown in figure 1(c), the background QWR is obviously wider than those of the

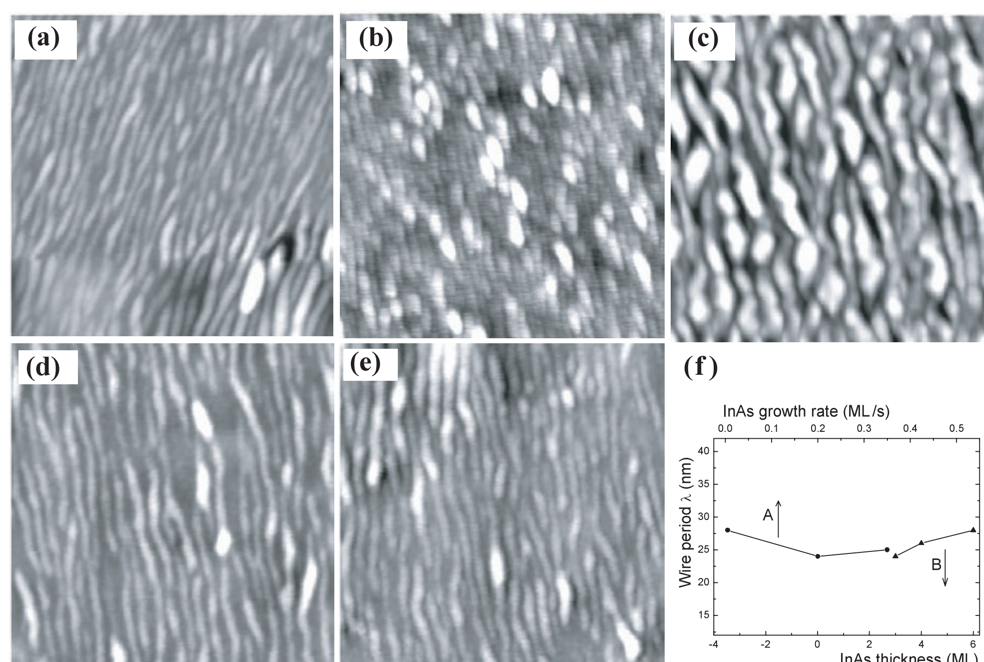

Figure 1. (a)–(e): AFM images of the InAs nanostructures grown on closely matched InAlAs/InP. (a)–(c): as a function of the InAs thickness with (a) 3 MLs, (b) 4 MLs, and (c) 6 MLs. The growth rate was 0.2 ML s^{-1}. (d) and (e): as a function of the InAs growth rate with (d) 0.005 ML s^{-1} and (e) 0.35 ML s^{-1}. The InAs layer thickness was 3 MLs. The size of the images is 0.5 μm $\times$ 0.5 μm. The elongated nanostructures are aligned along the $[1\bar{1}0]$ direction. (f) is the wire period λ as a function of growth rate with InAs coverage of 3 ML (arrow A) and deposition thickness with InAs growth rate of 0.2 ML s^{-1} (arrow B).

3 and 4 ML samples, and the bright QDs also have larger sizes than those of the 4 ML sample. Moreover, some QDs with a longer and irregular shape can be seen on some of the wires. Figures 1(d) and (e) show the morphologies of InAs nanostructures grown under different growth rates of 0.005 and 0.35 ML s^{-1} respectively. The samples have 3 MLs InAs thickness. Combined with figure 1(a), it is found that the self-organized structures formed under different growth rates all have a wire shape elongated along the $[1\bar{1}0]$ direction. In addition, elongated dots can be found on some of the wires for all the samples, which are usually wider than the wires.

Compared with the nanostructures formed on the InAs/GaAs system, in which variation of growth conditions will have a significant influence on the size, density, and distribution of the nanostructure [12–14], it seems that changing the InAs deposition and growth rate has little effect on the morphology and distribution of the nanostructures on InAlAs/InP. Statistics on the average pitch period λ of the wires are shown in figure 1(f), which indicates that the λ values range from 24 to 28 nm with only a small fluctuation under variant growth conditions. It is known that the formation of self-organized islands is closely related to epitaxial misfit and the accumulation of elastic strain in the epilayer. Therefore, the state of the InAlAs surface that directly interacts with the InAs layer is an important factor that needs to be considered.

3.1.2. Structural properties of InAlAs matrix layer. Figure 2 is a bright field plan-view TEM (H-9000 microscope) micrograph of an InAlAs layer. The electron beam is parallel

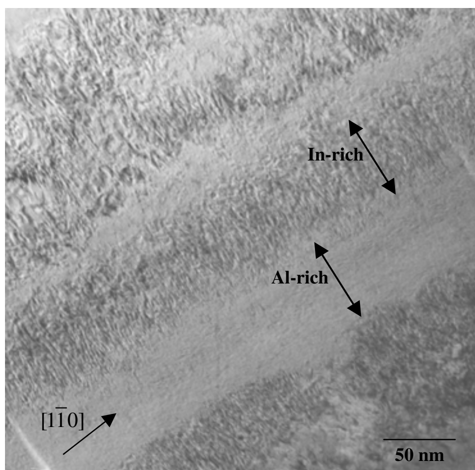

Figure 2. Plan-view TEM image of an InAlAs layer. The darker areas indicate In-rich regions, and the brighter areas indicate Al-rich regions.

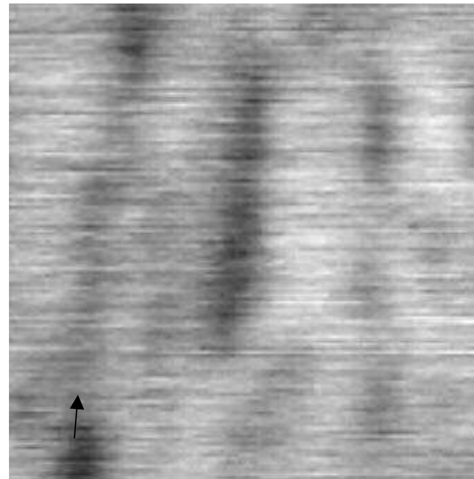

Figure 3. AFM image of an InAlAs surface without InAs deposition. The black arrow indicates the [1$\bar{1}$0] direction. The size of the images is 0.5 μm × 0.5 μm.

to the normal of the film surface. It is noted that strong contrast variations along the [110] direction exist, seen as alternate brighter and darker grey streaks. These streaks are elongated along the [1$\bar{1}$0] direction and are not very uniform in width, with the contrast modulation wavelength ranging from 45 to 130 nm. Energy dispersive x-ray spectrometry (EDX) was performed to investigate the origination of the contrast. According to the In atom content obtained from the EDX measurements, the In composition ranges are calculated to be 0.5 to 0.53 in the darker streaks and 0.46 to 0.48 in the brighter streaks. After all, the contrast is not constant within the darker or brighter streaks in figure 2. The alternate In-rich and In-poor (Al-rich) streaks mean that the LCM phenomenon has occurred in the InAlAs epilayer. On such a composition-modulated InAlAs layer, the press stress and the tensile stress in the In-rich and the Al-rich areas will lead to surface undulations [15], which have been evidenced by *in situ* reflection high energy electron diffraction (RHEED) observations. After deposition of 500 nm-thick InAlAs, the RHEED patterns are V-shaped spots along the [1$\bar{1}$0] direction and the superposition of streaks and spots along the [110] direction. The different RHEED patterns indicate the appearance of an elongated structure along the [1$\bar{1}$0] direction on the InAlAs surface [16]. Figure 3 presents a typical AFM image of an InAlAs surface, which shows obvious undulations elongated along the [1$\bar{1}$0] direction. The undulations are not very uniform; some undulations might coalesce or bifurcate. The height difference on the surface is less than 1.5 nm. The undulation wavelength obtained from a broad range of AFM images is from 50 to 140 nm, which is approximately equal to the modulation wavelength obtained from the TEM micrograph.

An important result from LCM is the in-plane optical anisotropy between [110] and [1$\bar{1}$0] in the vicinity of the band gap, which has been observed for MOCVD-grown InAlAs samples or InAlAs epilayers with InAs/AlAs short period superlattices [17, 18]. Here we adopt reflectance difference spectroscopy (RDS) to measure the reflectance difference of InAlAs epilayers along two perpendicular directions in the surface plane, i.e., $(r_{110} - r_{1\bar{1}0})/(r_{110} + r_{1\bar{1}0})$ [19]. Here r_{110} and $r_{1\bar{1}0}$ denote the reflectance for light polarized along the [110] and [1$\bar{1}$0] directions, respectively. The results measured at room temperature are shown in figure 4. The apparent resonant structures between 1.38 and 1.52 eV are attributed to the InAlAs band gap, while the

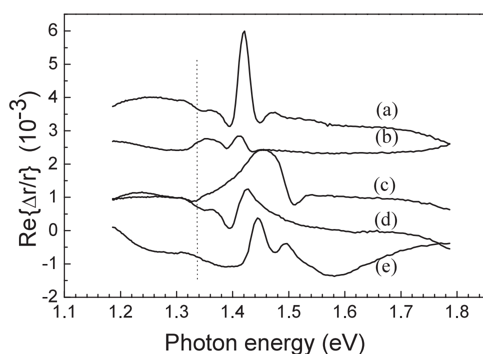

Figure 4. RD spectra of an InAlAs layer measured at room temperature. Spectra (a)–(e) correspond to InAlAs layer of samples sequentially shown in figures 1(a)–(e).

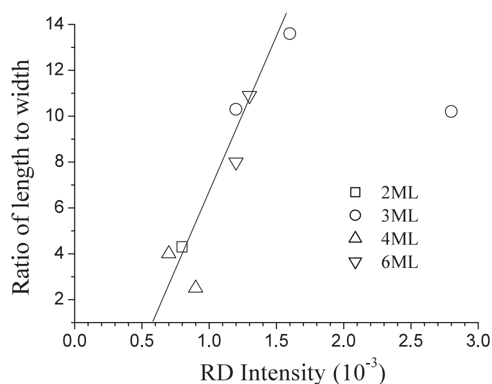

Figure 5. The ratio of the length to the width of the InAs wire-like structures formed under variant deposition thickness as a function of the RD intensity of InAlAs layer underlying the corresponding InAs layer.

small structures at 1.34 eV, indicating by a dashed line, are related to the InP band gap. It is known that Cu–Pt ordering can also cause the optical anisotropy between [110] and $[1\bar{1}0]$ directions [20, 21]. TEM and electron diffraction measurements show that there is no Cu–Pt ordering in our InAlAs samples, therefore we believe the observed optical anisotropy mainly comes from the LCM effect. The variation in the energy positions of the InAlAs-related structures indicates the different residual biaxial strain in the InAlAs layers. Actually the InAlAs layers were evidenced slightly compressed or tensed with a magnitude of $(\Delta a/a)_z$ less than 2×10^{-3} depending upon the samples by x-ray double crystal diffraction (XRD) measurements. In addition, this residual biaxial strain also leads to the splitting of the heavy- and light-hole band, which can be observed in the RD spectra if the splitting is large enough (for example, curves (c) and (e) in figure 4). From careful simulation of the RD spectra, one can obtain the residual biaxial strain components and an effective shear strain ε_{xy} that arises from LCM. This is beyond the scope of this paper and will be discussed elsewhere.

From AFM and RDS measurements, a close correlation between the RD intensity of InAlAs and the morphology parameters of the InAs nanostructures is established. Figure 5 illustrates the ratio of the length to the width of the InAs wire-like structures as a function of the RD intensity of the InAlAs layers. Apparently, as an increase in RD intensity of InAlAs, the InAs nanostructures on the InAlAs surface tend to have an elongated shape. Since the RD signal here is related to the LCM in InAlAs, this result directly confirms that the formation of the wire-like islands on the InAlAs surfaces is controlled by the LCM in InAlAs; that is why the formation of this wire-like structure is insensitive to the growth condition of InAs. In addition, the guide line in figure 5, which indicates the variation trend of the aspect ratio of the QWRs with the RD intensity, predicts that the shape of the self-assembled nanostructures will probably become isotropic when the RD intensity is about 6×10^{-4}. We guess that this RD signal of 6×10^{-4} results from residual shear strain in the InAlAs layers. Unlike LCM, which shows nanoscale patterns that can control the formation of QWRs as discussed later, the residual shear strain exhibits no direct relation with the formation of QWRs. The large deviation of the point (2.8×10^{-4}, 10.5) from the other points probably indicates a saturated effect of LCM on the elongation of the QWRs. Larger RD intensity reflects a stronger composition modulation in the LCM, but not necessarily a longer LCM in the surface plane. When the length of the QWRs becomes comparable to that of the LCM in the surface plane, the QWRs will not be

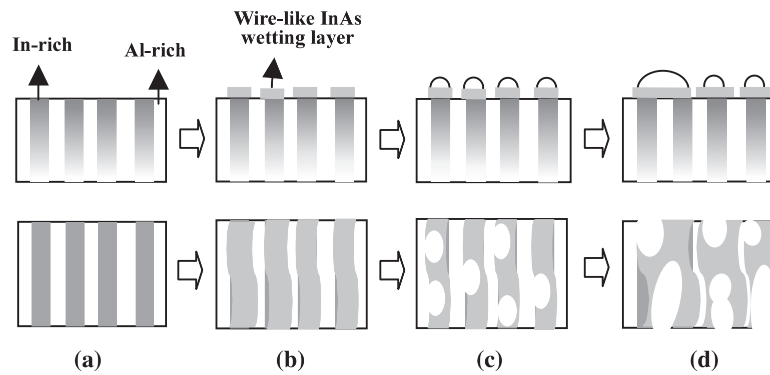

Figure 6. Schematic diagram of the modified SK growth mode that occurs on a composition modulation surface: (a) composition-modulated InAlAs layer, (b) wire-like InAs wetting layer formed on top of the In-rich areas, (c) elongated QDs formed on the wire-like InAs wetting layer, (d) coalescence of wire-like wetting layer and QDs respectively. The first row is the cross-section view; the second row is the top view.

elongated further even if the composition modulation is creased further. A full understanding of the figure 5 needs further researches on the correlation between the LCM in InAlAs and the RD intensity.

3.1.3. A picture of modified SK growth mode on a composition-modulated surface. On a composition-modulated InAlAs layer the surface lattice constant is also modulated. When InAs is deposited, it will preferentially settle down on the In-rich areas because of the lower misfit strain energy [15] and form [110]-oriented periodical undulations under the strain regulation. From this point of view, we propose a modified SK growth mode, shown in figure 6. First, at the initial stage of InAs deposition, wire-like wetting layers, instead of a planar wetting layer covering the whole substrate surface, are formed on the In-rich areas. The sizes of the wetting layers might not be uniform due to the nonuniformity of the composition modulation. Then, as more InAs is deposited, the accumulated elastic strain in the wire-like wetting layer becomes strong. An SK transition occurs on the wire-like wetting layer, causing the QDs to relax the excess strain. Meanwhile, the number of QDs would increase with increasing layer thickness. Finally, if the InAs coverage goes on increasing, the initially formed wire-like wetting layer might coalesce and become wider; thus its lateral domination on the QDs is weakened. Here, newly created QDs on the wider wire-like wetting layer might not be strictly aligned along the $[1\bar{1}0]$ direction. The coalescence of QDs with different orientation on the wires leads to the formation of larger and longer dots having irregular shape. We think that this growth mode is energetically favourable if the growth occurs on a composition-modulated layer. In this case, the pitch period λ of the wire-like wetting layer is expected to approximately equal the modulation wavelength of the InAlAs layer. However, we also note that the nonuniform strain distribution of the LCM will also lead to a surface undulation, which was indeed observed in our experiments. It is believed that the composition modulation can couple with a surface undulation with identical wavelength or one half wavelength [22]. The combined effect of the LCM and surface undulation will probably lead to the formation of InAs QWRs with the pitch period λ being one half of the wavelength of the LCM. That is probably the reason for the discrepancy between the λ value of the InAs QWRs, about 25 nm for all samples, and the wavelength of LCM, ranging from 45 to 130 nm. Another reason for the discrepancy may come

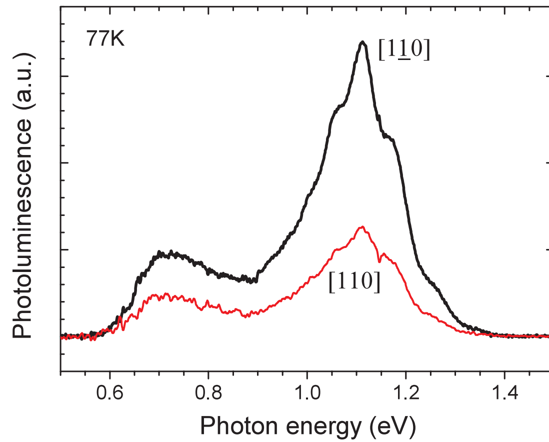

Figure 7. Polarized photoluminescence spectra at 77 K of InAs/InAlAs nanostructures. The InAs thickness is 3 ML and the growth rate is 0.2 ML s^{-1}.

(This figure is in colour only in the electronic version)

from the measurements from the different samples. Due to weak composition modulation in our samples, no LCM is clearly observed by cross-sectional TEM measurements. Therefore it is impossible to compare the pitch period λ of the QWRs with the LCM wavelength in the same samples. More effort is needed to clarify the discrepancy.

3.2. Optical properties of InAs nanostructures

The above modified SK growth mode can be confirmed further by the polarized photoluminescence (PL) measurements performed at 77 K. Figure 7 shows the polarized PL spectra of a sample with InAs growth rate of 0.2 ML s^{-1} and deposition thickness of 3 MLs. The spectra present a typically double-peak structure with a low-energy peak located at 0.71 eV and high-energy peak centred at 1.11 eV. The full width at half maximum (FWHM) for the high-energy peak is about 50 meV larger than that for the low-energy peak, which indicates a different origination of these two peaks. The PL polarization degree, $P = (I_{[1\bar{1}0]} - I_{[110]})/(I_{[1\bar{1}0]} + I_{[110]})$, is 38% and 45% for the low-energy peak and high-energy peak respectively. For other samples, the P of the lower-energy peak can be as small as 27%, while that of high-energy peak is up to 90%. In terms of the polarization degree and the peak position, the high-energy peak can be attributed to the wire-like wetting layer, and the low-energy peak can be attributed to the elongated QDs on the wetting layers. We see that, compared with the luminescence of the conventional planar wetting layer (see [23]), the luminescence of the wire-like wetting layer is of similar energy position but much higher optical anisotropy. The splitting of the spectra in the high-energy range stems from the monolayer height fluctuations of the wires [24]. In addition, the relative intensities of the two peaks also reflect the fact that for the 3 MLs InAs thickness the dot density is relatively small, thus the luminescence is dominated by the wire-like wetting layer.

It is known that the LCM phenomenon can be easily achieved in an InGaAs layer by growing an $(InAs)_m/(GaAs)_n$ short-period superlattice (SPS) [25, 26]. Therefore, growing an $(InAs)_m/(AlAs)_n$ SPS is expected to be a good way to clearly observe the modified SK growth mode of InAs nanostructures on an InAlAs layer.

4. Conclusions

In summary, we observe the lateral composition modulation phenomenon in heteroepitaxial lattice matched InAlAs films using TEM and find a close relation between the InAlAs RD intensity, which can represent the anisotropy magnitude of InAlAs layer, and the morphology evolution of the InAs nanostructure. On the lateral composition-modulated InAlAs matrix layer, the subsequently growing InAs film adopts a modified SK growth mode, in which wire-like wetting layers are first formed and then QDs are formed on the wire-like wetting layers. Moreover, with the increase of the deposition thickness, the wire-like wetting layer and the QDs will coalesce respectively. The PL measurements show that the luminescence of the wire-like wetting layer has similar peak position to the planar wetting layer but a large polarization degree. Furthermore, the wire-like wetting layer can provide direct control of the confined region for the future formed QDs, which demonstrates the possibility of producing controllable one-dimensional ordering QDs by growing them on a composition-modulated material.

Acknowledgments

The above work was supported by Special Funds for Major State Basic Research Project of China (No. G2000068303), National Natural Science Foundation of China (No. 60390071, 60390074, 60276014, 90101004, 90201033), and National High Technology Research and Development Program of China (No. 2002AA311070, 2002AA311170).

References

[1] Horikoshi Y, Yamaguchi H, Briones F and Kawashima M 1990 *J. Cryst. Growth* **105** 326
[2] García J M, González L, González M U, Silveira J P, González Y and Briones F 2001 *J. Cryst. Growth* **227** 975
[3] Cotta M A, Hamm R A, Staley T W, Chu S N G, Harriott L R and Panish M B 1993 *Phys. Rev. Lett.* **70** 4106
[4] Brault J, Gendry M, Grenet G, Hollinger G, Dieres Y and Benyattou T 1998 *Appl. Phys. Lett.* **73** 2932
[5] Zhang Z H, Pickrell G W, Chang K L, Lin H C, Hsieh K C and Cheng K Y 2003 *Appl. Phys. Lett.* **82** 4555
[6] Brault J, Gendry M, Grenet G, Hollinger G, Olivares J, Salem B, Benyattou T and Bremond G 2002 *J. Appl. Phys.* **92** 506
[7] Pashley M D 1989 *Phys. Rev.* B **40** 10481
[8] Shiraishi K 1992 *Appl. Phys. Lett.* **60** 1363
[9] Shin B, Lin A, Lappo K, Goldman R S, Hanna M C, Francoeur S, Norman A G and Mascarenhas A 2002 *Appl. Phys. Lett.* **80** 3292
[10] Cho H K, Lee J Y, Kwon M S, Lee B, Baek J-H and Han W S 1999 *Mater. Sci. Eng.* B **64** 174
[11] Glas F 1987 *J. Appl. Phys.* **62** 3201
[12] Westwood D I, Sobiesierski Z and Matthai C C 1999 *Appl. Surf. Sci.* **144/145** 484
[13] Joyce P B, Krzyzewski T J, Bell G R, Jones T S, Malik S, Childs D and Murray R 2001 *J. Cryst. Growth* **227/228** 1000
[14] Songmuang R, Kiravittaya S and Schmidt O G 2003 *J. Cryst. Growth* **249** 416
[15] Wohlert D E, Cheng K Y, Chang K L and Hsieh K C 1999 *J. Vac. Sci. Technol.* B **17** 1120
[16] Koo B H, Hanada T, Makino H, Chang J H and Yao T 2001 *J. Cryst. Growth* **229** 142
[17] Francoeur S, Zhang Y, Norman A G, Alsina F, Mascarenhas A, Reno J L, Jones E D, Lee S R and Follstaedt D M 2000 *Appl. Phys. Lett.* **77** 1765
[18] Francoeur S, Hanna M C, Norman A G and Mascarenhas A 2002 *Appl. Phys. Lett.* **80** 243
[19] Aspnes D E, Harbison J P, Studna A A and Folrez L T 1988 *J. Vac. Sci. Technol.* A **6** 1327
[20] Su L C, Ho I H, Kobayashi N and Stringfellow G B 1994 *J. Cryst. Growth* **145** 140
[21] Ernst P, Zhang Yong, Driessen F A J M, Mascarenhas A, Jones E D, Geng C, Scholz F and Schweizer H 1997 *J. Appl. Phys.* **81** 2815
[22] Glas F 2000 *Phys. Rev.* B **62** 7393
[23] Li H X, Wu J, Xu B, Liang J B and Wang Z G 1998 *Appl. Phys. Lett.* **72** 2123
[24] Carlin J F, Houdré R, Rudra A and llegems M 1991 *Appl. Phys. Lett.* **59** 3018
[25] Cheng K Y, Hsieh K C and Baillargeion J N 1992 *Appl. Phys. Lett.* **60** 2892
[26] Chou S T, Cheng K Y, Chou L J and Hsieh K C 1995 *J. Appl. Phys.* **78** 6270